Journal of Mathematical Modeling
Vol. -, No. -, 2026, pp. -. Research Article

Fractional-order models of species interaction: solitary wave and analytical dynamics

F. Ahmadi Ghavibazoo[†], H. Mesgarani[†*], M. Garshasbi[§]

[†]*Department of Mathematics, Faculty of Science, Shahid Rajaee Teacher Training University, Tehran, 16785 -136, I. R. Iran*
[§]*School of Mathematics & Computer Sciences, Iran University of Science & Technology, Tehran, Iran*

Email(s): fahmadighavibazoo@sru.ac.ir, hmesgarani@sru.ac.ir, m_garshasbi@iust.ac.ir

Abstract. We derive explicit traveling-wave and solitary-wave solutions for a coupled fractional reaction–diffusion system describing interacting populations. The analytical framework combines a rational–exponential ansatz with an auxiliary-function expansion, where the auxiliary function satisfies a linear second-order ordinary differential equation. Time- and space-fractional derivatives, defined in the sense of Jumarie's modified Riemann–Liouville derivative, are incorporated through a fractional complex transformation that reduces the governing fractional partial differential system to an ordinary differential system. A homogeneous-balance procedure yields algebraic relations whose solutions generate several families of closed-form expressions, including hyperbolic, rational, and oscillatory wave profiles classified according to the discriminant of the auxiliary equation. The obtained solutions demonstrate how the fractional-order parameters influence wave propagation, localization, and diffusion behavior, providing additional insight beyond the corresponding classical integer-order model. Representative graphical illustrations together with symbolic verification confirm the validity of the analytical solutions and demonstrate the applicability of the proposed framework for studying nonlinear fractional reaction–diffusion systems.

Keywords: Fractional differential equations, soliton solutions, traveling waves, reaction–diffusion, variable-order fractional derivatives.
AMS Subject Classification 2010: 35R11, 35C07, 34A34

1 Introduction

Fractional differential equations (FDEs) extend classical integer–order models by incorporating nonlocal memory effects, which are crucial for describing real-world systems with hereditary and anomalous

*Corresponding author
Received: 29 October 2025/ Revised: 13 July 2026/ Accepted: 13 July 2026
DOI: 10.22124/jmm.2026.32115.2902

transport behaviors [4, 16, 23]. In recent years, fractional calculus has gained increasing attention for modeling complex processes in biological populations, viscoelastic materials, fluid dynamics, and astrophysical systems [19, 21, 34]. Unlike integer-order models, fractional frameworks capture long-term memory and spatial heterogeneity, both of which play a central role in realistic dynamic systems.

Recent studies have demonstrated the relevance of fractional reaction–diffusion equations in describing biological and chemical interactions with nonlocal memory [8,20,27]. These models generalize the classical reaction–diffusion paradigm by including time- and space-fractional derivatives, thereby providing a more accurate description of anomalous diffusion and dispersal patterns. Analytical advances, such as those by Mahmoud [20] and Sarwe et al. [27], have highlighted the feasibility of obtaining closed-form and approximate solutions for fractional systems with variable coefficients.

Various analytical methods have been developed to solve nonlinear FDEs, including perturbation approaches, the homotopy analysis and homotopy perturbation methods [9], Hirota's bilinear formulation [12], the $\frac{G'}{G}$–expansion technique [2,3,6,24,33], and the Exp–function method [25,30,32,35]. These methods provide systematic tools for constructing exact traveling-wave solutions that reveal the structure and propagation mechanisms of nonlinear waves. Moreover, recent numerical frameworks, such as collocation and finite-difference schemes for fractional systems [26], complement analytical developments by providing accurate simulations for nonlocal diffusion processes.

In ecological and biological contexts, fractional reaction–diffusion models have proven effective for describing spatial dispersal, invasion fronts, and pattern formation [1, 18, 22, 28]. Skellam's pioneering work established that random dispersal combined with exponential growth produces linearly expanding population fronts, while subsequent studies have revealed nonlinear effects, such as density dependence and Allee thresholds, that slow or even halt propagation [18, 22]. The inclusion of fractional derivatives extends these insights by accounting for anomalous migration, long-range dispersal, and memory-driven diffusion [1, 8].

Motivated by these considerations, this study aims to derive analytical traveling-wave and solitary-wave solutions for a coupled nonlinear fractional reaction–diffusion system modeling interacting populations. In contrast to the corresponding integer-order formulation, the fractional model incorporates memory effects and anomalous diffusion, allowing a broader class of wave structures and providing a more flexible description of population dispersal dynamics. By employing Jumarie's modified Riemann–Liouville fractional derivative together with a fractional complex transformation and both the Exp–function and $\frac{G'}{G}$–expansion methods, explicit families of traveling-wave solutions are obtained. The modified Riemann–Liouville derivative is adopted because it is well suited for describing non-smooth physical quantities frequently encountered in biological and diffusion processes while preserving convenient analytical properties that facilitate the application of exact solution methods. These characteristics make it an appropriate choice for the analytical treatment considered in the present work.

Moreover, Jumarie's derivative preserves several familiar and useful properties of classical calculus, including linearity, the derivative of a constant being zero, a modified product rule, and a chain-rule-type property. These features make analytical techniques, such as the Exp–function method and the $\frac{G'}{G}$–expansion method, more straightforward to apply within the framework of the present paper. The obtained solutions are classified into hyperbolic, rational, and oscillatory families according to the discriminant of the auxiliary equation. This classification provides a systematic characterization of the admissible wave structures and facilitates comparison with the corresponding classical reaction–diffusion model. Graphical illustrations are presented to demonstrate the qualitative behavior of the obtained solutions.

The remainder of this paper is structured as follows. Section 2 formally states the problem. Section 3 introduces the analytical framework and the transformation techniques employed in the study. Section 4 presents specific model applications along with the corresponding parameter selections. Section 5 concludes the paper by summarizing the main findings and outlining potential directions for future research on fractional population models.

2 Problem definition

In this section, we introduce a coupled fractional reaction–diffusion system that models the dynamics of interacting populations. To formulate the system, we employ Jumarie's modified Riemann–Liouville fractional derivative, which is well suited for handling non-differentiable population profiles [13–15]. When species invasion is examined in more complex ecological settings involving interspecific interactions, most existing extensions focus primarily on pairwise competition. Under such conditions, a system of coupled partial differential equations is typically used to describe the spatial spread of two competing species [11]. In this study, the classical coupled reaction–diffusion model is generalized by introducing both time- and space-fractional derivatives, thereby incorporating memory effects and anomalous diffusion into the interaction dynamics:

$$\begin{cases} D_t^{\alpha_t} u = \mathscr{D}_u D_x^{\alpha_x} u + \left(\rho_u - \gamma_{uu} u - \gamma_{uv} v\right) u, \\ D_t^{\alpha_t} v = \mathscr{D}_v D_x^{\alpha_x} v + \left(\rho_v - \gamma_{vv} v - \gamma_{vu} u\right) v, \end{cases} \tag{1}$$

where $u(x,t)$ and $v(x,t)$ denote the densities of the two species, $\mathscr{D}_u$ and $\mathscr{D}_v$ are species-specific diffusion rates, ρ_u and ρ_v are species-specific intrinsic rates of increase, γ_{uv} and γ_{vu} denote interspecific competition coefficients, whereas γ_{uu} and γ_{vv} denote intraspecific competition coefficients. In this equation, $D_t^{\alpha_t}$ and $D_x^{\alpha_x}$ denote the time- and space-fractional derivatives of orders $0 < \alpha_t \leq 1$ and $0 < \alpha_x \leq 1$, respectively. For $\alpha_t = \alpha_x = 1$, system (1) reduces to the corresponding classical reaction–diffusion model. Consequently, the fractional orders extend the classical formulation by incorporating memory effects and anomalous diffusion, while preserving the integer-order model as a limiting case.

Remark on dimensional consistency. The introduction of fractional derivatives modifies the physical dimensions of the governing equations. In particular, the temporal fractional derivative $D_t^{\alpha_t}$ has the effective dimension $T^{-\alpha_t}$, whereas the spatial fractional derivative $D_x^{\alpha_x}$ has the effective dimension $L^{-\alpha_x}$. To preserve dimensional consistency, the model parameters are interpreted as effective fractional coefficients whose dimensions depend on the corresponding fractional orders. Accordingly, the intrinsic growth-rate parameters ρ_u and ρ_v possess the effective dimension $T^{-\alpha_t}$, while the effective fractional diffusion coefficients $\mathscr{D}_u$ and $\mathscr{D}_v$ possess the effective dimension $L^{\alpha_x} T^{-\alpha_t}$. Under this interpretation, every term in each equation of system (1) has the same physical dimension, ensuring the dimensional consistency of the fractional model. Throughout this work, the governing equations are therefore interpreted within this fractional-dimensional framework, following the standard practice adopted in the literature on fractional reaction–diffusion equations.
The modified Riemann–Liouville derivative is defined as follows [15, 24]:

$$D_t^{\alpha_t} f(t) = \frac{1}{\Gamma(1-\alpha_t)} \frac{d}{dt} \int_0^t (t-\xi)^{-\alpha_t} \left[f(\xi) - f(0)\right] d\xi, \qquad 0 < \alpha_t < 1. \tag{2}$$

Similarly, the modified Riemann–Liouville space-fractional derivative is defined by

$$D_x^{\alpha_x} f(x) = \frac{1}{\Gamma(1-\alpha_x)} \frac{d}{dx} \int_0^x (x-\xi)^{-\alpha_x} \left[f(\xi) - f(0) \right] d\xi, \qquad 0 < \alpha_x < 1, \tag{3}$$

where $\Gamma(\cdot)$ denotes the Gamma function. Throughout this paper, both the temporal derivative $D_t^{\alpha_t}$ and the spatial derivative $D_x^{\alpha_x}$ are understood in the modified Riemann–Liouville sense.
The time- and space-fractional derivatives differ only by the independent variable with respect to which the operator is taken; however, both are explicitly presented here for completeness and to avoid ambiguity in the formulation of the governing equations.
The following properties of Jumarie's modified Riemann–Liouville derivative will be used throughout the subsequent analysis.

$$D_t^{\alpha_t} t^r = \frac{\Gamma(1+r)}{\Gamma(1+r-\alpha_t)} t^{r-\alpha_t}, \tag{4}$$

$$D_t^{\alpha_t} (k f(t)) = k D_t^{\alpha_t} f(t), \tag{5}$$

$$D_t^{\alpha_t} (a f(t) + b g(t)) = a D_t^{\alpha_t} f(t) + b D_t^{\alpha_t} g(t), \tag{6}$$

where a, b, k are arbitrary constants.
Since the objective is the construction of exact traveling-wave solutions, the explicit forms of the initial and boundary conditions are not required in the subsequent analytical developments.

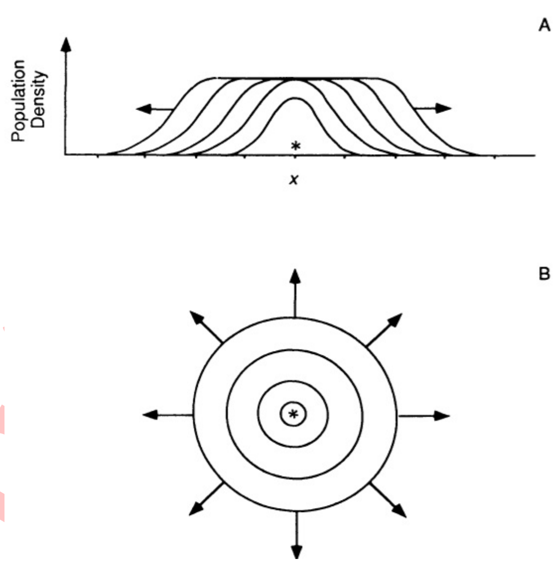

Figure 1: Representative traveling-wave solutions illustrating the dispersal of populations into unoccupied regions. (A) Sequential profiles of a one-dimensional wave propagating along a linear habitat (e.g., riverbank or coastline), with the initial release point marked by an asterisk. Each curve represents the population density along the x-axis at successive times. (B) A two-dimensional representation showing concentric patterns of population spread. Although the profiles resemble traveling waves, the wave profile remains unchanged while propagating through space.

3 Methods description

3.1 The fractional complex transform

The solution procedure consists of two main stages. First, the fractional complex transform is employed to reduce the governing fractional partial differential equations into a system of ordinary differential equations. Subsequently, the Exp-function method is applied to construct exact traveling-wave solutions of the resulting reduced system. This combination provides a systematic framework for obtaining explicit analytical solutions of nonlinear fractional reaction–diffusion equations.
We start with the following system of nonlinear fractional partial differential equations (FPDEs):

$$\mathscr{P}\left(u, D_t^{\alpha_t} u, D_x^{\alpha_x} u, \dots\right) = 0, \tag{7}$$

where $0 < \alpha_x, \alpha_t < 1$, u is an unknown function, and $\mathscr{P}$ is a polynomial in u and its fractional derivatives, in which the highest order derivatives and the nonlinear terms are involved. The fractional complex transform [17] was first proposed by Li and He in 2010 to convert the fractional differential equations with the modified Riemann–Liouville derivative into ordinary differential equations, which can be easily solved using simple calculus. Using the fractional complex transform, the traveling-wave variable is defined by

$$u(x,t) = U(\zeta), \qquad v(x,t) = V(\zeta), \qquad \zeta = \kappa_1 \frac{x^{\alpha_x}}{\Gamma(1+\alpha_x)} - \kappa_2 \frac{t^{\alpha_t}}{\Gamma(1+\alpha_t)}, \tag{8}$$

where α_x and α_t denote the fractional orders of the spatial and temporal derivatives, respectively, κ_1, κ_2 are scaling constants. Following the fractional complex transform proposed by Li and He and using Jumarie's modified Riemann–Liouville derivative, the fractional chain rule is assumed in the form

$$D_t^{\alpha_t} u = \frac{\partial U}{\partial \zeta} D_t^{\alpha_t} \zeta, \qquad D_t^{\alpha_t} v = \frac{\partial V}{\partial \zeta} D_t^{\alpha_t} \zeta, \qquad D_x^{\alpha_x} u = \frac{\partial U}{\partial \zeta} D_x^{\alpha_x} \zeta, \qquad D_x^{\alpha_x} v = \frac{\partial V}{\partial \zeta} D_x^{\alpha_x} \zeta. \tag{9}$$

It should be emphasized that the fractional chain rule employed in Eq. (9) is not generally valid for arbitrary definitions of fractional derivatives. In the present work, it is adopted exclusively within the framework of Jumarie's modified Riemann–Liouville derivative together with the fractional complex transform proposed by Li and He [17]. Under these assumptions, the transformation provides an effective analytical reduction of the considered fractional reaction–diffusion system to an ordinary differential system. Several authors have pointed out that generalized chain rules may fail outside specific fractional frameworks [7, 29]. Therefore, the validity of the present transformation should be understood as being restricted to the modified Riemann–Liouville derivative adopted throughout this paper, and no claim is made regarding its applicability to other fractional operators, such as the classical Riemann–Liouville or Caputo derivatives.
Using the properties of Jumarie's modified Riemann–Liouville derivative adopted in this work, one obtains

$$D_x^{\alpha_x}\left(\frac{x^{\alpha_x}}{\Gamma(1+\alpha_x)}\right) = 1, \qquad D_t^{\alpha_t}\left(\frac{t^{\alpha_t}}{\Gamma(1+\alpha_t)}\right) = 1. \tag{10}$$

Therefore, from the travelling-wave variable

$$\zeta = \kappa_1 \frac{x^{\alpha_x}}{\Gamma(1+\alpha_x)} - \kappa_2 \frac{t^{\alpha_t}}{\Gamma(1+\alpha_t)}. \tag{11}$$

It follows that

$$D_x^{\alpha_x} \zeta = \kappa_1, \qquad D_t^{\alpha_t} \zeta = -\kappa_2. \tag{12}$$

Applying the fractional chain rule in Eq. (9), we obtain

$$D_t^{\alpha_t} u = \frac{dU}{d\zeta} D_t^{\alpha_t} \zeta = -\kappa_2 U', \qquad D_x^{\alpha_x} u = \frac{dU}{d\zeta} D_x^{\alpha_x} \zeta = \kappa_1 U', \tag{13}$$

and similarly

$$D_t^{\alpha_t} v = \frac{dV}{d\zeta} D_t^{\alpha_t} \zeta = -\kappa_2 V', \qquad D_x^{\alpha_x} v = \frac{dV}{d\zeta} D_x^{\alpha_x} \zeta = \kappa_1 V'. \tag{14}$$

Substituting these expressions into the fractional reaction–diffusion system

$$D_t^{\alpha_t} u = \mathscr{D}_u D_x^{\alpha_x} u + (\rho_u - \gamma_{uu} u - \gamma_{uv} v) u, \tag{15}$$

$$D_t^{\alpha_t} v = \mathscr{D}_v D_x^{\alpha_x} v + (\rho_v - \gamma_{vv} v - \gamma_{vu} u) v, \tag{16}$$

and using the travelling-wave transformations $u(x,t) = U(\zeta)$ and $v(x,t) = V(\zeta)$, we obtain
Each fractional derivative is replaced by its corresponding expression in terms of the travelling-wave variable ζ, after which like terms are collected to obtain the reduced ordinary differential system.

$$-\kappa_2 U' = \mathscr{D}_u \kappa_1 U' + (\rho_u - \gamma_{uu} U - \gamma_{uv} V) U, \tag{17}$$
$$-\kappa_2 V' = \mathscr{D}_v \kappa_1 V' + (\rho_v - \gamma_{vv} V - \gamma_{vu} U) V. \tag{18}$$

After rearranging terms, the original fractional partial differential system is reduced to the following coupled system of ordinary differential equations:

$$\begin{cases} (\kappa_2 + \kappa_1 \mathscr{D}_u) U'(\zeta) + \rho_u U - \gamma_{uu} U^2 - \gamma_{uv} UV = 0, \\ (\kappa_2 + \kappa_1 \mathscr{D}_v) V'(\zeta) + \rho_v V - \gamma_{vv} V^2 - \gamma_{vu} UV = 0. \end{cases} \tag{19}$$

Hence, the fractional complex transform successfully converts the original fractional-order system into a coupled system of ordinary differential equations with respect to the travelling-wave variable ζ. The resulting system can then be analyzed by employing the Exp-function method to derive exact traveling-wave solutions.

3.2 The Exp-function method for FPDEs

We start with the following system of nonlinear FPDEs:

$$\mathscr{P}\left(u, v, D_t^{\alpha_t} u, D_t^{\alpha_t} v, D_x^{\alpha_x} u, D_x^{\alpha_x} v, \dots\right) = 0, \tag{20}$$

where $0 < \alpha_x, \alpha_t < 1$, u is an unknown function, and $\mathscr{P}$ is a polynomial in u and its fractional derivatives, in which the highest order derivatives and the nonlinear terms are involved. The fractional complex transform [17] was first proposed by Li and He in 2010 to convert the fractional differential equations with the modified Riemann–Liouville derivative into ordinary differential equations, which can be easily solved using simple calculus. Using the fractional complex transform, the traveling-wave variable is defined by

$$u(x,t) = U(\zeta), \qquad v(x,t) = V(\zeta), \qquad \zeta = \kappa_1 \frac{x^{\alpha_x}}{\Gamma(1+\alpha_x)} - \kappa_2 \frac{t^{\alpha_t}}{\Gamma(1+\alpha_t)}, \tag{21}$$

where α_x and α_t denote the fractional orders of the spatial and temporal derivatives, respectively, κ_1, κ_2 are scaling constants. The positive integer q of the solution is determined via a balancing procedure, by equating the highest-order derivative with the leading nonlinear term.
Specifically, for $D[U(\zeta)] = q$,

$$D\Big[\frac{d^p U}{d\zeta^p}\Big] = p+q, \qquad D\Big[U^m\Big(\frac{d^r U}{d\zeta^r}\Big)^s\Big] = mq + s(q+r),$$

ensuring consistency between linear and nonlinear contributions. If necessary, the resulting ODE can be simplified through direct integration. Assume that each component admits a finite rational–exponential representation:

$$U(\zeta) = \frac{\sum_{m=-M}^{M} a_m e^{m\zeta}}{\sum_{n=-N}^{N} b_n e^{n\zeta}}, \qquad V(\zeta) = \frac{\sum_{m=-M}^{M} c_m e^{m\zeta}}{\sum_{n=-N}^{N} d_n e^{n\zeta}},$$

with a_m, b_n, c_m, d_n as constants and integers M, N fixed by homogeneous balancing of the highest derivatives versus the highest nonlinearities in (19). Substituting these forms into the ODEs, collecting like powers of $e^{\ell\zeta}$, and equating the corresponding coefficients produces a finite algebraic system for the unknown coefficients a_m, b_n, c_m, d_n together with the wave parameters. Solving this algebraic system symbolically or numerically yields explicit parameter sets and closed-form expressions for $U(\zeta)$ and $V(\zeta)$.
The determination of the balance numbers in the Exp–function method is based on the homogeneous balance principle. Depending on the structure of the nonlinear ordinary differential equation, the following balance rules are commonly employed [5, 18]:

1. **Homogeneous balance principle 1.** If $U^{(p)}$ and $U^{(\rho)}$ denote the leading linear and dominant nonlinear terms, then balancing yields $c_1 = c_2$ and $d_1 = d_2$ for all $p, \rho \geq 1$.

2. **Homogeneous balance principle 2.** For nonlinear ODEs containing $U^{(p)}$ and $U^k U^{(r)}$ as the main terms, the balance relation remains $c_1 = c_2$ and $d_1 = d_2$ for all $p, r, k \geq 1$.

3. **Homogeneous balance principle 3.** If $U^{(p)}$ and $(U^{(r)})^{\Omega}$ constitute the leading linear and nonlinear components, then the same balancing yields $c_1 = c_2$ and $d_1 = d_2$ for all $p, r \geq 1$ and $\Omega \geq 2$.

4. **Homogeneous balance principle 4.** When $U^{(p)}$ and nonlinear terms of the form $(U^{(r)})^{\Omega} U^{(\lambda)}$ appear, one similarly obtains $c_1 = c_2$ and $d_1 = d_2$ for $p, r, \lambda \geq 1$ and $\Omega \geq 2$.

In the present work, the first balance principle is applicable since the reduced system contains first-order derivative terms and quadratic nonlinearities. Consequently, balancing U' with U^2 and V' with V^2 yields the balance numbers used in the subsequent analysis. For system (19), the highest-order linear terms are the first derivatives $U'(\zeta)$ and $V'(\zeta)$, whereas the dominant nonlinear terms are $U^2(\zeta)$ and $V^2(\zeta)$. Applying the first homogeneous balance principle gives

$$M = N = 1,$$

which determines the orders of the numerator and denominator in the Exp–function ansatz adopted throughout the subsequent analysis.

3.3 The rational $(\frac{G'}{G})$-expansion method for FPDEs

We consider a coupled system of nonlinear fractional partial differential equations involving the independent variables (x) and (t) of the form

$$\mathscr{F}\left(u_i, \frac{\partial u_i}{\partial t}, \frac{\partial u_i}{\partial x}, D_t^{\alpha_t} u_i, D_x^{\alpha_x} u_i, \dots\right) = 0, \qquad i = 1, 2, \tag{22}$$

where $(u_1 = u)$ and $(u_2 = v)$ denote the dependent variables, and $(\mathscr{F})$ is a polynomial function involving the dependent variables and their integer- and fractional-order derivatives. The rational $\frac{G'}{G}$–expansion method proceeds as follows:

Step 1: Fractional traveling-wave reduction

The fractional complex transform is widely used to convert fractional partial differential equations into ordinary differential equations through a traveling-wave reduction. Introduce a traveling-wave coordinate ζ defined as [10, 17, 31]:

$$\zeta = \kappa_1 \frac{x^{\alpha_x}}{\Gamma(1+\alpha_x)} - \kappa_2 \frac{t^{\alpha_t}}{\Gamma(1+\alpha_t)}, \tag{23}$$

where (α_x) and (α_t) denote the orders of the space- and time-fractional derivatives, respectively, and (κ_1) and (κ_2) are arbitrary scaling constants.
Also, assuming that each field variable depends solely on ζ

$$u_i(t, x_1, x_2, \dots, x_n) = U_i(\zeta), \quad \zeta = \zeta(t, x_1, x_2, \dots, x_n).$$

Although the method is stated in a general multidimensional setting, the model considered in this work is one-dimensional with independent variables (x, t).
Using the extended fractional complex transform, Eq. (23), we convert the fractional differential system into an ordinary differential system in ζ, thereby transforming the original fractional system into a system of ordinary differential equations with respect to the traveling-wave variable ζ.

The original FDE reduces to an ODE in ζ

$$\mathscr{Q}(U_i, U_i', U_i'', \dots) = 0, \tag{24}$$

where primes denote derivatives with respect to ζ.

Step 2: Rational $\left(\frac{G'}{G}\right)$ ansatz

The following procedure is presented for a generic dependent variable $U(\zeta)$. The same construction can be applied to each component of the coupled system. The solution of Eq. (24) is assumed in the rational form:

$$U(\zeta) = \frac{\sum_{j=0}^{N_1} a_j \left(\frac{G'}{G}\right)^j}{\sum_{j=0}^{N_2} b_j \left(\frac{G'}{G}\right)^j}, \tag{25}$$

where a_j and b_j are real constants, with at least one nonzero coefficient among the highest-order terms, and $G(\zeta)$ satisfies a linear auxiliary equation:

$$G''(\zeta) + \Lambda G'(\zeta) + M\, G(\zeta) = 0, \tag{26}$$

with constants Λ, M.

Step 3: Solution of the linear auxiliary ODE

Let $\Delta = \sqrt{\Lambda^2 - 4M}$ and $\Omega = \sqrt{4M - \Lambda^2}$. The general solution of Eq. (26) gives

$$\left(\frac{G'}{G}\right) = \begin{cases} -\frac{\Lambda}{2} + \frac{\Delta}{2}\,\dfrac{C_1 \sinh\left(\frac{\Delta}{2}\zeta\right) + C_2 \cosh\left(\frac{\Delta}{2}\zeta\right)}{C_1 \cosh\left(\frac{\Delta}{2}\zeta\right) + C_2 \sinh\left(\frac{\Delta}{2}\zeta\right)}, & \Lambda^2 > 4M, \\ -\frac{\Lambda}{2} + \frac{\Omega}{2}\,\dfrac{-C_1 \sin\left(\frac{\Omega}{2}\zeta\right) + C_2 \cos\left(\frac{\Omega}{2}\zeta\right)}{C_1 \cos\left(\frac{\Omega}{2}\zeta\right) + C_2 \sin\left(\frac{\Omega}{2}\zeta\right)}, & \Lambda^2 < 4M, \\ -\frac{\Lambda}{2} + \dfrac{C_2}{C_1 + C_2\zeta}, & \Lambda^2 = 4M, \end{cases} \tag{27}$$

with arbitrary constants C_1 and C_2.

Step 4: Parameter determination

The integers N_1 and N_2 are determined using the homogeneous balance principle, which equates the highest derivative with the leading nonlinear term. Substituting the ansatz and $\frac{G'}{G}$ into the ODE produces a polynomial in $\frac{G'}{G}$, and setting each coefficient to zero yields a system of algebraic equations for the coefficients a_j $(j = 0, \ldots, N_1)$, b_j $(j = 0, \ldots, N_2)$, and the parameters Λ and M.

Step 5: Solution construction

The resulting algebraic system is solved symbolically using *Mathematica*. The obtained parameter sets are then substituted into the rational $\left(\frac{G'}{G}\right)$-ansatz together with the corresponding auxiliary-function solutions to derive explicit closed-form traveling-wave and solitary-wave solutions of the original nonlinear fractional differential equations.

4 Results

4.1 Closed-form solutions via the rational $\frac{G'}{G}$–expansion method

To construct explicit solitary-wave solutions for the system in Eq. (1), we employ the rational $\frac{G'}{G}$–expansion method.
Using the homogeneous balance principle, the highest powers N_1 and N_2 are determined from the reduced system (19).
Here, balancing U' with U^2 and V' with V^2 gives

$$N_1 = N_2 = 1.$$

We then seek solutions of the original reduced system in the form

$$U(\zeta) = a_0 + a_1 \frac{G'(\zeta)}{G(\zeta)}, \qquad V(\zeta) = b_0 + b_1 \frac{G'(\zeta)}{G(\zeta)}, \tag{28}$$

where a_0, a_1, b_0, b_1 are constants to be determined.
Substitute (28) into (19) and use (26) to express derivatives of $\frac{G'}{G}$ in closed form. Collect terms by powers of $\frac{G'}{G}$ (and constants) and set coefficients to zero; the resulting algebraic relations determine $(a_0, a_1, b_0, b_1, \Lambda, M)$ in terms of system parameters $(\rho_i, \gamma_{ij}, i, j = u, v)$. corresponding to $\Lambda^2 > 4M$, $\Lambda^2 = 4M$, and $\Lambda^2 < 4M$ give rise to hyperbolic, rational, or oscillatory closed-form expressions for $U(\zeta)$ and $V(\zeta)$.
The homogeneous-balance principle applied to (19) indicates that a linear dependence on $\frac{G'}{G}$ suffices (i.e., a first-order ansatz in (28)). Substituting Eq. (28) into Eq. (19) and collecting coefficients of like powers of $\frac{G'}{G}$ yields the following algebraic system:

$$\begin{aligned}
&-(\kappa_2 + \kappa_1 \mathscr{D}_u)a_1 - \gamma_{uu} a_1^2 - \gamma_{uv} a_1 b_1 = 0,\\
&-(\kappa_2 + \kappa_1 \mathscr{D}_u)\Lambda a_1 + \rho_u a_1 - 2\gamma_{uu} a_0 a_1 - \gamma_{uv} a_0 b_1 - \gamma_{uv} a_1 b_0 = 0,\\
&-(\kappa_2 + \kappa_1 \mathscr{D}_u)M a_1 + \rho_u a_0 - \gamma_{uu} a_0^2 - \gamma_{uv} a_0 b_0 = 0,\\
&-(\kappa_2 + \kappa_1 \mathscr{D}_v)b_1 - \gamma_{vv} b_1^2 - \gamma_{vu} a_1 b_1 = 0,\\
&-(\kappa_2 + \kappa_1 \mathscr{D}_v)\Lambda b_1 + \rho_v b_1 - 2\gamma_{vv} b_0 b_1 - \gamma_{vu} a_0 b_1 - \gamma_{vu} a_1 b_0 = 0,\\
&-(\kappa_2 + \kappa_1 \mathscr{D}_v)M b_1 + \rho_v b_0 - \gamma_{vv} b_0^2 - \gamma_{vu} a_0 b_0 = 0.
\end{aligned} \tag{29}$$

The algebraic system (29) was solved symbolically using *Mathematica*, yielding admissible parameter sets and the corresponding exact traveling-wave solution families. Representative families of exact solutions obtained from these parameter sets are presented below.

Solution branches

The symbolic solution of the algebraic system (29) obtained using *Mathematica* leads to several admissible parameter branches. Each branch satisfies the algebraic constraints and generates a distinct family of exact traveling-wave solutions. These branches are analyzed below.

Case 1. Eq. (29) admits a solution branch characterized by

$$\gamma_{vv} = 0, \qquad \gamma_{uv} = 0, \qquad \rho_v = 0, \qquad a_0 = 0,$$

$$\gamma_{vu}\,\kappa_1 \neq 0, \qquad \gamma_{vu}\,b_1 \neq 0, \qquad \gamma_{uu} \neq 0,$$

$$\mathscr{D}_u = \frac{\mathscr{D}_v\,\gamma_{uu}\,\kappa_1 + \gamma_{uu}\,\kappa_2 - \gamma_{vu}\,\kappa_2}{\gamma_{vu}\,\kappa_1}, \qquad \mathscr{D}_v = \frac{-\kappa_2}{\kappa_1}$$

$$a_1 = \frac{-\mathscr{D}_u\,\kappa_1 - \kappa_2}{\gamma_{uu}},$$

with b_0, b_1, κ_1, and κ_2 being arbitrary parameters satisfying the above constraints.
Case 2. Eq. (29) admits a further solution branch characterized by

$$\gamma_{uu} \neq 0, \quad \kappa_1 \neq 0, \quad \gamma_{vv} \neq 0, \quad \gamma_{uv} = 0,$$

$$\mathscr{D}_u = \frac{-\kappa_2}{\kappa_1}, \quad \mathscr{D}_v = \frac{-\kappa_2}{\kappa_1}, \quad a_0 = \frac{\rho_u}{\gamma_{uu}}, \quad a_1 = \frac{-\mathscr{D}_u\,\kappa_1 - \kappa_2}{\gamma_{uu}},$$

$$b_0 = \frac{-\gamma_{vu}\rho_u + \gamma_{uu}\rho_v}{\gamma_{uu}\gamma_{vv}}, \qquad b_1 = \frac{-a_1\gamma_{vu} - \mathscr{D}_v\,\kappa_1 - \kappa_2}{\gamma_{vv}},$$

with ρ_u, ρ_v, Λ, κ_1, and κ_2 being arbitrary parameters satisfying the above constraints.
Case 3. Eq. (29) admits a further solution branch defined by

$$\kappa_1 \neq 0, \quad b_1 = 0, \quad \gamma_{uu}\,\gamma_{vv}\,(-\gamma_{uv}\,\gamma_{vu} + \gamma_{uu}\,\gamma_{vv}) \neq 0, \quad \gamma_{vu} \neq 0,$$

$$a_0 = \frac{-b_0\,\gamma_{vv} + \rho_v}{\gamma_{vu}}, \qquad a_1 = \frac{-\mathscr{D}_u\,\kappa_1 - \kappa_2}{\gamma_{uu}},$$

$$b_0 = \frac{\rho_v}{\gamma_{vv}}, \qquad \mathscr{D}_u = -\frac{\kappa_2}{\kappa_1},$$

with ρ_u, ρ_v, κ_1, and κ_2 being arbitrary parameters satisfying the above constraints.
Case 4. Eq. (29) admits another solution branch characterized by

$$\rho_u = 0, \quad \rho_v = 0, \quad \gamma_{uv} = 0, \qquad \gamma_{vv} = 0,$$

$$\kappa_2 M \neq 0, \quad \gamma_{uu} \neq 0, \quad \gamma_{vu} \neq 0,$$

$$a_1 = -\frac{\kappa_2}{\gamma_{uu}}, \quad a_0 = -\frac{\kappa_2\Lambda}{2\gamma_{vu}},$$

$$b_0 = \frac{\Lambda}{2}\,b_1, \quad \Lambda = \pm 2\sqrt{M},$$

with M, b_1, κ_1 and κ_2 being arbitrary parameters satisfying the above constraints. The corresponding solutions are

Exact solitary-wave solutions

For illustration, we focus on Case 1, which yields representative solitary-wave solutions.
For **Case 1**, with $\Lambda^2 - 4M > 0$, the solutions take the form

$$U_1(\zeta) = -\frac{\mathscr{D}_u \kappa_1 + \kappa_2}{\gamma_{uu}} \left[-\frac{\Lambda}{2} + \frac{\Delta}{2} \frac{C_1 \sinh\left(\frac{\Delta}{2}\zeta\right) + C_2 \cosh\left(\frac{\Delta}{2}\zeta\right)}{C_1 \cosh\left(\frac{\Delta}{2}\zeta\right) + C_2 \sinh\left(\frac{\Delta}{2}\zeta\right)} \right], \tag{30}$$

$$V_1(\zeta) = b_0 + b_1 \left[-\frac{\Lambda}{2} + \frac{\Delta}{2} \frac{C_1 \sinh\left(\frac{\Delta}{2}\zeta\right) + C_2 \cosh\left(\frac{\Delta}{2}\zeta\right)}{C_1 \cosh\left(\frac{\Delta}{2}\zeta\right) + C_2 \sinh\left(\frac{\Delta}{2}\zeta\right)} \right]. \tag{31}$$

If $\Lambda^2 - 4M = 0$,

$$U_2(\zeta) = -\frac{\mathscr{D}_u \kappa_1 + \kappa_2}{\gamma_{uu}} \left[-\frac{\Lambda}{2} + \frac{C_2}{C_1 + C_2\zeta} \right], \tag{32}$$

$$V_2(\zeta) = b_0 + b_1 \left[-\frac{\Lambda}{2} + \frac{C_2}{C_1 + C_2\zeta} \right]. \tag{33}$$

Finally if $\Lambda^2 - 4M < 0$,

$$U_3(\zeta) = -\frac{\mathscr{D}_u \kappa_1 + \kappa_2}{\gamma_{uu}} \left[-\frac{\Lambda}{2} + \frac{\Omega}{2} \frac{-C_1 \sin\left(\frac{\Omega}{2}\zeta\right) + C_2 \cos\left(\frac{\Omega}{2}\zeta\right)}{C_1 \cos\left(\frac{\Omega}{2}\zeta\right) + C_2 \sin\left(\frac{\Omega}{2}\zeta\right)} \right], \tag{34}$$

$$V_3(\zeta) = b_0 + b_1 \left[-\frac{\Lambda}{2} + \frac{\Omega}{2} \frac{-C_1 \sin\left(\frac{\Omega}{2}\zeta\right) + C_2 \cos\left(\frac{\Omega}{2}\zeta\right)}{C_1 \cos\left(\frac{\Omega}{2}\zeta\right) + C_2 \sin\left(\frac{\Omega}{2}\zeta\right)} \right]. \tag{35}$$

To illustrate the influence of the fractional orders and model parameters on the obtained traveling-wave solutions, two- and three-dimensional plots are presented in Figures 2–8. The parameters α_t and α_x denote the orders of the temporal and spatial fractional derivatives, respectively. For visualization purposes, the analytical solutions are expressed in terms of the physical variables x and t through the traveling-wave transformation.
Figures 2–4 present the two- and three-dimensional profiles of the solutions $V_1(\zeta)$, $V_2(\zeta)$, and $V_3(\zeta)$ corresponding to the three cases $\Lambda^2 - 4M > 0$, $\Lambda^2 - 4M = 0$, and $\Lambda^2 - 4M < 0$, respectively. The graphical results clearly indicate that the qualitative behavior of the traveling-wave solutions is highly sensitive to the sign of the discriminant $\Lambda^2 - 4M$, leading to distinctly different wave structures in each case. The presented figures illustrate the traveling-wave profiles corresponding to the selected parameter values listed in Tables 1–3. The qualitative behavior of the solutions depends on the sign of the discriminant $\Lambda^2 - 4M$, which leads to hyperbolic, rational, and oscillatory wave structures.
To investigate the effect of the fractional-order parameter, the solutions are also plotted for

$$\alpha = \alpha_t = \alpha_x = 0.3,\ 0.5,\ 0.7,\ 0.9,$$

while all remaining parameters are fixed at the values listed in the corresponding tables. This enables a direct comparison of the influence of the fractional order on the traveling-wave profiles. To verify the obtained solutions, each solution family was substituted symbolically into the reduced system (19) using *Mathematica*. The resulting residuals vanish identically, confirming that the derived expressions satisfy the reduced system exactly.

4.1.1 Biological significance of the fractional-order parameters

The fractional orders α_t and α_x provide a natural way to incorporate memory and nonlocal interactions into the present species-interaction model. The temporal fractional order α_t characterizes the strength of the memory effect in the population dynamics. Smaller values of α_t indicate that the current growth and interaction rates are more strongly influenced by the past states of the populations, whereas values approaching the corresponding classical (integer-order) dynamics.
Similarly, the spatial fractional order α_x describes the degree of nonlocal dispersal. Lower values of α_x represent anomalous diffusion, where individuals may perform long-range movements or disperse through heterogeneous environments, while $\alpha_x = 1$ recovers the classical local diffusion process.
In the numerical illustrations, the representative values $\alpha = 0.3$, 0.5, 0.7, and 0.9 are selected to demonstrate different biological regimes ranging from strong memory and pronounced nonlocal transport to weak memory and nearly classical diffusion. These values are not intended to represent a specific ecological system, but rather to illustrate how variations in the fractional orders affect the propagation speed, localization, and shape of the traveling-wave solutions. Consequently, decreasing the fractional orders leads to slower wave propagation and broader wave fronts due to enhanced memory and nonlocal effects, whereas increasing the orders towards unity results in faster propagation and wave profiles approaching those of the corresponding classical reaction–diffusion model

4.2 Verification of the obtained $\frac{G'}{G}$-expansion solutions

To verify the correctness of the obtained analytical solutions, each solution family derived by the $\frac{G'}{G}$-expansion method was substituted into the reduced algebraic system obtained from the coefficient comparison. The corresponding algebraic residuals are defined by

$$\begin{aligned}
R_1 &= -(\kappa_2 + \kappa_1 \mathscr{D}_u)a_1 - \gamma_{uu}a_1^2 - \gamma_{uv}a_1b_1, \\
R_2 &= -(\kappa_2 + \kappa_1 \mathscr{D}_u)\Lambda a_1 + \rho_u a_1 - 2\gamma_{uu}a_0a_1 - \gamma_{uv}a_0b_1 - \gamma_{uv}a_1b_0, \\
R_3 &= -(\kappa_2 + \kappa_1 \mathscr{D}_u)Ma_1 + \rho_u a_0 - \gamma_{uu}a_0^2 - \gamma_{uv}a_0b_0, \\
R_4 &= -(\kappa_2 + \kappa_1 \mathscr{D}_v)b_1 - \gamma_{vv}b_1^2 - \gamma_{vu}a_1b_1, \\
R_5 &= -(\kappa_2 + \kappa_1 \mathscr{D}_v)\Lambda b_1 + \rho_v b_1 - 2\gamma_{vv}b_0b_1 - \gamma_{vu}a_0b_1 - \gamma_{vu}a_1b_0, \\
R_6 &= -(\kappa_2 + \kappa_1 \mathscr{D}_v)Mb_1 + \rho_v b_0 - \gamma_{vv}b_0^2 - \gamma_{vu}a_0b_0.
\end{aligned} \tag{36}$$

For each admissible parameter set reported in Section 4, the corresponding parameter constraints were substituted into R_i $(i = 1, \ldots, 6)$. Symbolic simplification using *Mathematica* yielded

$$R_1 = R_2 = R_3 = R_4 = R_5 = R_6 \equiv 0,$$

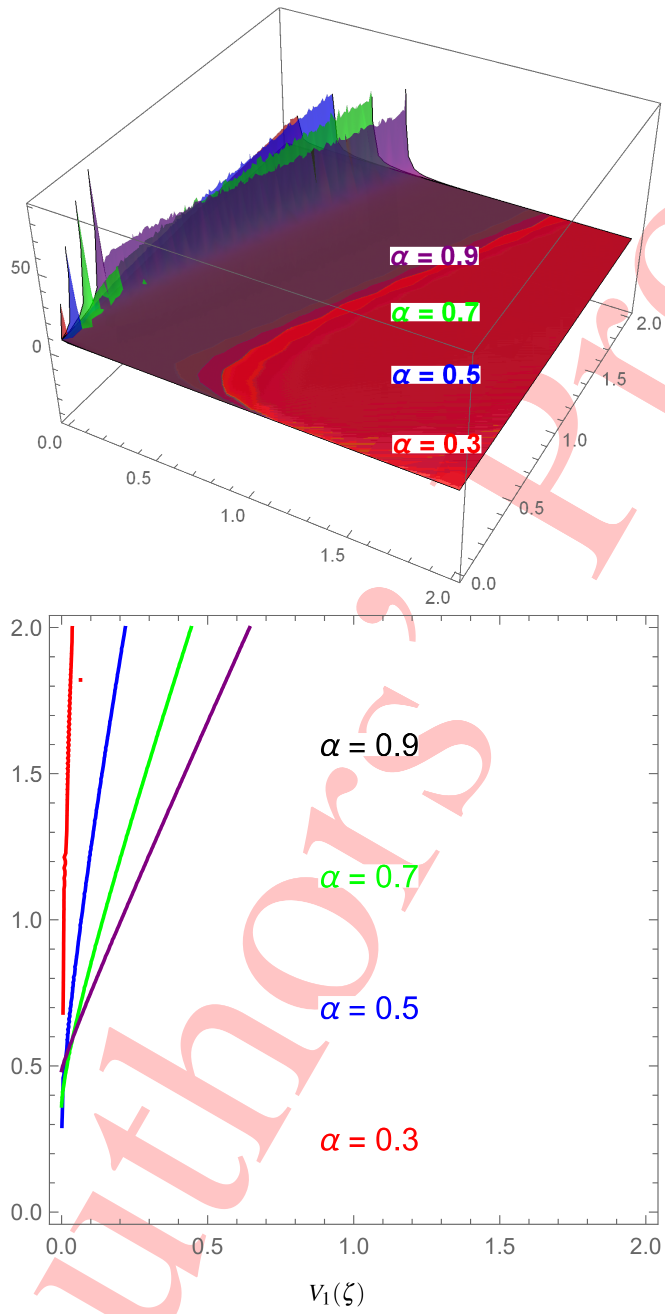

Figure 2: Two- and three-dimensional profiles of the solution $V_1(\zeta)$ corresponding to the parameter values listed in Table 1 for the case $\Lambda^2 - 4M > 0$.

Table 1: Parameter values used in Figure 2

Parameter	α_t	α_x	b_0	b_1	γ_{uu}	γ_{vu}	C_1	C_2	ρ_u	κ_1	κ_2	Λ	M	x	t
Value	0.5	0.5	7	0.75	0.7	0.9	2	3	0.8	2	1	5	2	$(0,5)$	$(0,5)$

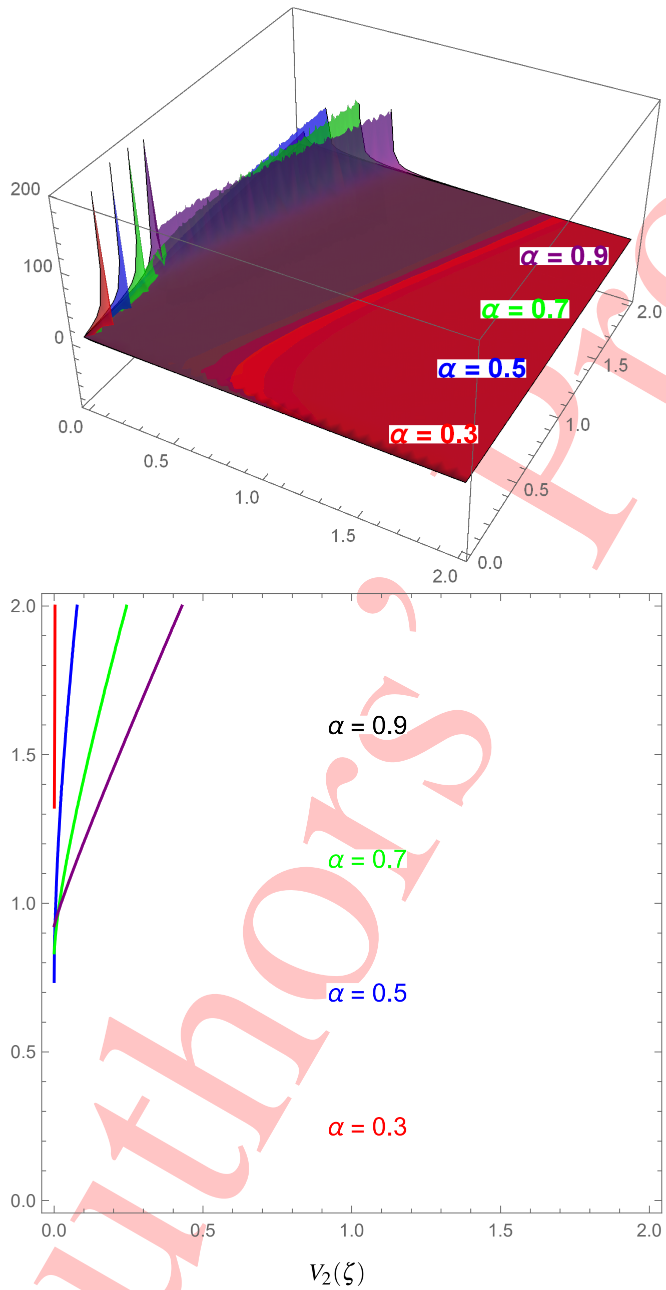

Figure 3: Two- and three-dimensional profiles of the solution $V_2(\zeta)$ corresponding to the parameter values listed in Table 2 for the case $\Lambda^2 - 4M = 0$.

Table 2: Parameter values used in Figure 3

Parameter	α_t	α_x	b_0	b_1	γ_{uu}	γ_{vu}	C_1	C_2	ρ_u	κ_1	κ_2	Λ	M	x	t
Value	0.5	0.5	7	0.75	0.7	0.9	2	3	0.8	2	1	4	4	$(0,5)$	$(0,5)$

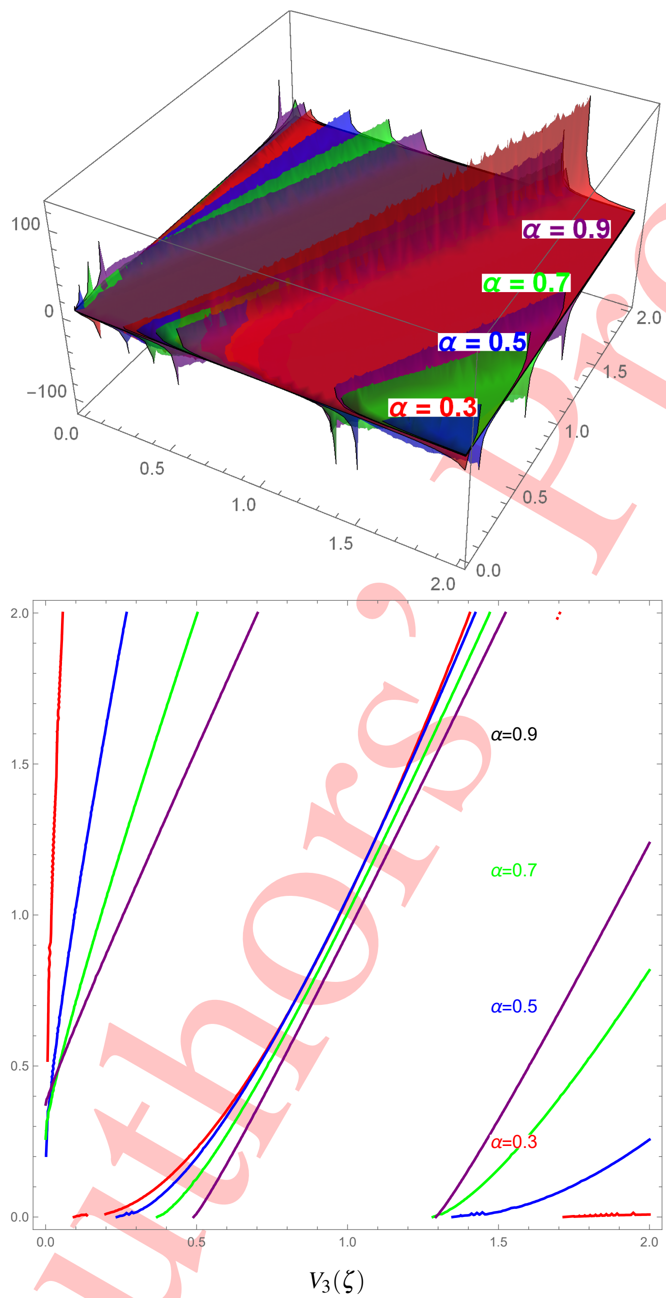

Figure 4: Two- and three-dimensional profiles of the solution $V_3(\zeta)$ corresponding to the parameter values listed in Table 3 for the case $\Lambda^2 - 4M < 0$.

Table 3: Parameter values used in Figure 4

Parameter	α_t	α_x	b_0	b_1	γ_{uu}	γ_{vu}	C_1	C_2	ρ_u	κ_1	κ_2	Λ	M	x	t
Value	0.5	0.5	7	0.75	0.7	0.9	2	3	0.8	2	1	3	4	$(0,5)$	$(0,5)$

which is equivalent to the symbolic output

$$\{\text{True}, \text{True}, \text{True}, \text{True}, \text{True}, \text{True}\}.$$

Furthermore, the obtained expressions $U(\zeta)$ and $V(\zeta)$ were substituted into the original fractional reaction–diffusion system (1), and the corresponding differential residuals were defined by

$$R_u = D_t^{\alpha_t} u - \mathscr{D}_u D_x^{\alpha_x} u - (\rho_u - \gamma_{uu} u - \gamma_{uv} v)u,$$

$$R_v = D_t^{\alpha_t} v - \mathscr{D}_v D_x^{\alpha_x} v - (\rho_v - \gamma_{vv} v - \gamma_{vu} u)v.$$

After symbolic simplification in *Mathematica*, both residuals vanished identically,

$$R_u \equiv 0, \qquad R_v \equiv 0.$$

Therefore, the obtained closed-form solutions satisfy not only the reduced algebraic system but also the original fractional reaction–diffusion equations exactly, confirming the correctness and internal consistency of the derived solutions.

4.3 Closed-form solutions of the main problem using the Exp–function method

To construct explicit solitary-wave solutions for the reduced system (19), we employ the Exp–function method. The highest-order derivative terms $U'(\zeta)$ and $V'(\zeta)$ are balanced against the dominant nonlinear terms $U^2(\zeta)$ and $V^2(\zeta)$. Consequently, the homogeneous balance procedure yields

$$M = N = 1.$$

Accordingly, the Exp–function ansatz is chosen as

$$U(\zeta) = \frac{a_{-1}e^{-\zeta} + a_0 + a_1 e^{\zeta}}{b_{-1}e^{-\zeta} + b_0 + b_1 e^{\zeta}}, \qquad V(\zeta) = \frac{c_{-1}e^{-\zeta} + c_0 + c_1 e^{\zeta}}{d_{-1}e^{-\zeta} + d_0 + d_1 e^{\zeta}}. \tag{37}$$

Substituting the ansatz (37) into the reduced system (19), multiplying both equations by the corresponding denominator polynomials, and expanding the resulting expressions produce polynomials in e^{ζ}. Collecting the coefficients of the linearly independent powers $e^{n\zeta}$ $(n = -3, -2, \dots, 3)$ and setting each coefficient equal to zero yield a coupled nonlinear algebraic system for the unknown coefficients

$$a_i,\ b_i,\ c_i,\ d_i, \qquad (i = -1, 0, 1).$$

The resulting algebraic system is solved symbolically using *Mathematica*. Since the intermediate symbolic expansions are lengthy and do not provide additional analytical insight, they are omitted for brevity, whereas the complete nonlinear algebraic system is presented below. The reported equations can be reproduced directly by following the above symbolic procedure.
By applying the above symbolic procedure to the first equation of the reduced system (19), the following nonlinear algebraic system is obtained:

$$
\begin{aligned}
&\rho_u a_{-1}b_{-1}d_{-1}-\gamma_{uu}a_{-1}^2 d_{-1}-\gamma_{uv}a_{-1}b_{-1}c_{-1}=0,\\
&\rho_u a_{-1}b_{-1}d_0+\rho_u a_{-1}b_0 d_{-1}+\rho_u a_0 b_{-1}d_{-1}-\gamma_{uu}a_{-1}^2 d_0-2\gamma_{uu}a_{-1}a_0 d_{-1}-\gamma_{uv}a_{-1}c_{-1}b_0\\
&\quad-\gamma_{uv}a_0 b_{-1}c_{-1}-\gamma_{uv}a_{-1}c_0 b_{-1}-(\kappa_2+\kappa_1\mathscr{D}_u)a_{-1}b_0 d_{-1}+(\kappa_2+\kappa_1\mathscr{D}_u)b_{-1}a_0 d_{-1}=0,\\
&\rho_u a_{-1}b_{-1}d_1+\rho_u a_{-1}b_0 d_0+\rho_u a_{-1}b_1 d_{-1}+\rho_u a_0 b_{-1}d_0+\rho_u a_0 b_0 d_{-1}+\rho_u a_1 b_{-1}d_{-1}\\
&\quad-\gamma_{uu}a_{-1}^2 d_1-\gamma_{uu}a_0^2 d_{-1}-2\gamma_{uu}a_{-1}a_0 d_0-2\gamma_{uu}a_{-1}a_1 d_{-1}-(\kappa_2+\kappa_1\mathscr{D}_u)a_{-1}b_0 d_0\\
&\quad+(\kappa_2+\kappa_1\mathscr{D}_u)b_{-1}a_0 d_0-2(\kappa_2+\kappa_1\mathscr{D}_u)a_{-1}b_1 d_{-1}+2(\kappa_2+\kappa_1\mathscr{D}_u)a_1 b_{-1}d_{-1}=0,\\
&\rho_u a_{-1}b_0 d_1+\rho_u a_{-1}b_1 d_0+\rho_u a_0 b_{-1}d_1+\rho_u a_0 b_0 d_0+\rho_u a_0 b_1 d_{-1}+\rho_u a_1 b_{-1}d_0+\rho_u a_1 b_0 d_{-1}\\
&\quad-2\gamma_{uu}a_{-1}a_0 d_1-2\gamma_{uu}a_{-1}a_1 d_0-\gamma_{uu}a_0^2 d_0-2\gamma_{uu}a_0 a_1 d_{-1}-\gamma_{uv}c_{-1}a_0 b_1-\gamma_{uv}c_0 a_{-1}b_1-\gamma_{uv}c_{-1}a_1 b_0\\
&\quad-\gamma_{uv}c_0 a_0 b_0-\gamma_{uv}c_1 a_{-1}b_0-\gamma_{uv}c_0 a_1 b_{-1}-\gamma_{uv}c_1 a_0 b_{-1}-(\kappa_2+\kappa_1\mathscr{D}_u)a_{-1}b_0 d_1\\
&\quad+(\kappa_2+\kappa_1\mathscr{D}_u)a_0 b_{-1}d_1-2(\kappa_2+\kappa_1\mathscr{D}_u)a_{-1}b_1 d_0+2(\kappa_2+\kappa_1\mathscr{D}_u)a_1 b_{-1}d_0=0,\\
&\rho_u a_{-1}b_1 d_1+\rho_u a_0 b_0 d_1+\rho_u a_0 b_1 d_0+\rho_u a_1 b_{-1}d_1+\rho_u a_1 b_0 d_0+\rho_u a_1 b_1 d_{-1}\\
&\quad-2\gamma_{uu}a_{-1}a_1 d_1-\gamma_{uu}a_0^2 d_1-2\gamma_{uu}a_0 a_1 d_0-\gamma_{uu}a_1^2 d_{-1}-\gamma_{uv}a_1 c_{-1}b_1-\gamma_{uv}a_0 c_0 b_{-1}\\
&\quad-\gamma_{uv}a_0 c_0 b_1-\gamma_{uv}a_{-1}c_1 b_1-\gamma_{uv}a_1 c_0 b_0-\gamma_{uv}a_0 c_1 b_0-\gamma_{uv}a_1 c_1 b_{-1}-2(\kappa_2+\kappa_1\mathscr{D}_u)a_{-1}b_1 d_1\\
&\quad+2(\kappa_2+\kappa_1\mathscr{D}_u)a_1 b_{-1}d_1+(\kappa_2+\kappa_1\mathscr{D}_u)a_1 b_0 d_0+(\kappa_2+\kappa_1\mathscr{D}_u)a_1 b_0 d_1-(\kappa_2+\kappa_1\mathscr{D}_u)a_0 b_1 d_0=0,\\
&\rho_u a_0 b_1 d_1+\rho_u a_1 b_0 d_1+\rho_u a_1 b_1 d_0-2\gamma_{uu}a_0 a_1 d_1-\gamma_{uu}a_1^2 d_0-\gamma_{uv}a_1 c_1 b_0-\gamma_{uv}a_1 c_0 b_1-\gamma_{uv}a_0 c_1 b_1=0,\\
&\rho_u a_1 b_1 d_1-\gamma_{uu}a_1^2 d_1-\gamma_{uv}a_1 b_1 c_1=0.
\end{aligned}
$$

Applying the same symbolic procedure to the second equation of the reduced system (19) yields the following nonlinear algebraic system:

$$
\begin{aligned}
&-\gamma_{vv}c_{-1}^2 b_{-1}-\gamma_{vu}a_{-1}c_{-1}d_{-1}+\rho_v c_{-1}d_{-1}b_{-1}=0,\\
&\rho_v c_{-1}b_{-1}d_0+\rho_v c_{-1}b_0 d_{-1}+\rho_v c_0 b_{-1}d_{-1}-\gamma_{vv}c_{-1}^2 b_0-2\gamma_{vv}c_{-1}c_0 b_{-1}-\gamma_{vu}a_{-1}c_{-1}d_0\\
&\quad-\gamma_{vu}a_0 c_{-1}d_{-1}-\gamma_{vu}a_{-1}c_0 d_{-1}-(\kappa_2+\kappa_1\mathscr{D}_v)c_{-1}d_0 b_{-1}+(\kappa_2+\kappa_1\mathscr{D}_v)d_{-1}c_0 b_{-1}=0,\\
&\rho_v c_{-1}b_{-1}d_1+\rho_v c_{-1}b_0 d_0+\rho_v c_{-1}b_1 d_{-1}+\rho_v c_0 b_{-1}d_0+\rho_v c_0 b_0 d_{-1}+\rho_v c_1 b_{-1}d_{-1}\\
&\quad-\gamma_{vv}c_{-1}^2 b_1-2\gamma_{vv}c_{-1}c_0 b_0-2\gamma_{vv}c_{-1}c_1 b_{-1}-\gamma_{vv}c_0^2 b_{-1}-\gamma_{vu}a_{-1}c_{-1}d_1-\gamma_{vu}a_0 c_{-1}d_0\\
&\quad-\gamma_{vu}a_{-1}c_0 d_0-\gamma_{vu}a_1 c_{-1}d_{-1}-\gamma_{vu}a_0 c_0 d_{-1}-\gamma_{vu}a_{-1}c_1 d_{-1}-(\kappa_2+\kappa_1\mathscr{D}_v)c_{-1}d_0 b_0\\
&\quad+(\kappa_2+\kappa_1\mathscr{D}_v)c_0 d_{-1}b_0-2(\kappa_2+\kappa_1\mathscr{D}_v)c_{-1}d_1 b_{-1}+2(\kappa_2+\kappa_1\mathscr{D}_v)c_1 d_{-1}b_{-1}=0,\\
&\rho_v c_{-1}b_0 d_1+\rho_v c_{-1}b_1 d_0+\rho_v c_0 b_{-1}d_1+\rho_v c_0 b_0 d_0+\rho_v c_0 b_1 d_{-1}+\rho_v c_1 b_{-1}d_0+\rho_v c_1 b_0 d_{-1}\\
&\quad-2\gamma_{vv}c_{-1}c_0 b_1-2\gamma_{vv}c_{-1}c_1 b_0-\gamma_{vv}c_0^2 b_0-2\gamma_{vv}c_0 c_1 b_{-1}-\gamma_{vu}a_0 c_{-1}d_1-\gamma_{vu}a_{-1}c_0 d_1\\
&\quad-\gamma_{vu}a_1 c_{-1}d_0-\gamma_{vu}a_0 c_0 d_0-\gamma_{vu}a_{-1}c_1 d_0-\gamma_{vu}a_1 c_0 d_{-1}-\gamma_{vu}a_0 c_1 d_{-1}-(\kappa_2+\kappa_1\mathscr{D}_v)c_{-1}d_0 b_1\\
&\quad+(\kappa_2+\kappa_1\mathscr{D}_v)c_0 d_{-1}b_1-2(\kappa_2+\kappa_1\mathscr{D}_v)c_{-1}d_1 b_0+2(\kappa_2+\kappa_1\mathscr{D}_v)c_1 d_{-1}b_0\\
&\quad+(\kappa_2+\kappa_1\mathscr{D}_v)c_1 d_0 b_{-1}-(\kappa_2+\kappa_1\mathscr{D}_v)c_0 d_1 b_{-1}=0,\\
&\rho_v c_{-1}b_1 d_1+\rho_v c_0 b_0 d_1+\rho_v c_0 b_1 d_0+\rho_v c_1 b_{-1}d_1+\rho_v c_1 b_0 d_0+\rho_v c_1 b_1 d_{-1}-2\gamma_{vv}c_{-1}c_1 b_1\\
&\quad-\gamma_{vv}c_0^2 b_1-2\gamma_{vv}c_0 c_1 b_0-\gamma_{vv}c_1^2 b_{-1}-\gamma_{vu}a_1 c_{-1}d_1-\gamma_{vu}a_0 c_0 d_1-\gamma_{vu}a_{-1}c_1 d_1\\
&\quad-\gamma_{vu}a_1 c_0 d_0-\gamma_{vu}a_0 c_1 d_0-\gamma_{vu}a_1 c_1 d_{-1}-2(\kappa_2+\kappa_1\mathscr{D}_v)c_{-1}d_1 b_1+2(\kappa_2+\kappa_1\mathscr{D}_v)c_1 d_{-1}b_1\\
&\quad+(\kappa_2+\kappa_1\mathscr{D}_v)c_1 d_0 b_0-(\kappa_2+\kappa_1\mathscr{D}_v)c_0 d_1 b_0=0,
\end{aligned}
\tag{38}
$$

$$
\begin{aligned}
&\rho_v c_0 b_1 d_1 + \rho_v c_1 b_1 d_0 + \rho_v c_1 b_0 d_1 - 2\gamma_{vv} c_0 c_1 b_1 - \gamma_{vv} c_1^2 b_0 - \gamma_{vu} a_1 c_0 d_1 - \gamma_{vu} a_0 c_1 d_1\\
&\quad - \gamma_{vu} a_1 c_1 d_0 - (\kappa_2 + \kappa_1 \mathscr{D}_v) c_0 d_1 b_1 + (\kappa_2 + \kappa_1 \mathscr{D}_v) c_1 d_0 b_1 = 0,\\
&\rho_v c_1 b_1 d_1 - \gamma_{vv} c_1^2 b_1 - \gamma_{vu} a_1 c_1 d_1 = 0.
\end{aligned}
$$

Solving the above nonlinear algebraic system symbolically yields several admissible solution branches corresponding to different parameter constraints. These branches are presented and discussed separately in the following cases.

Solving the nonlinear algebraic system (38) symbolically using *Mathematica* yields four admissible solution branches, each corresponding to a distinct set of parameter constraints. These solution branches are presented below.

Case 1. One admissible solution branch is obtained under the parameter constraints

$$
\gamma_{vv} = 0, \quad \gamma_{uv} = 0, \quad a_0 = 0, \quad \gamma_{uu}\kappa_1\rho_v \neq 0, \quad \gamma_{vu} \neq 0, \quad b_0 = 0,
$$

$$
b_1 c_1 d_1 \rho_u \neq 0, \quad d_{-1}(\mathscr{D}_v \kappa_1 + \kappa_2)\rho_u \neq 0, \quad a_{-1} c_{-1} \neq 0,
$$

$$
\begin{aligned}
\mathscr{D}_u &= \frac{\gamma_{vu}\rho_u^2 - \gamma_{uu}\kappa_2\rho_v}{\gamma_{uu}\kappa_1\rho_v},\\
\rho_u &= \frac{\rho_v \gamma_{uu}}{\gamma_{vu}}, \quad d_0 = \frac{c_0 d_{-1}}{c_{-1}},\\
a_1 &= \frac{b_1 \rho_u}{\gamma_{uu}}, \quad c_1 = \frac{c_{-1} d_1}{d_{-1}}, \quad b_{-1} = \frac{a_{-1}\gamma_{vu}}{\rho_v},
\end{aligned}
$$

with c_0, b_1, c_1, d_1, κ_1 and ρ_v arbitrary constants. The corresponding exact solutions are given by

$$
U_{(1,1)}(\zeta) = \frac{a_{-1}e^{-\zeta} + (\frac{b_1\rho_u}{\gamma_{uu}})e^{\zeta}}{(\frac{a_{-1}\gamma_{vu}}{\rho_v})e^{-\zeta} + b_1 e^{\zeta}}, \qquad V_{(1,1)}(\zeta) = \frac{c_{-1}e^{-\zeta} + c_0 + (\frac{c_{-1}d_1}{d_{-1}})e^{\zeta}}{d_{-1}e^{-\zeta} + (\frac{c_0 d_{-1}}{c_{-1}}) + d_1 e^{\zeta}}.
$$

Case 2. Another admissible solution branch is obtained for

$$
b_0 = 0, \quad d_0 = 0, \quad a_0 = 0, \quad c_{-1} = 0, \quad d_1 = 0,
$$

$$
\gamma_{uv} = 0, \quad \gamma_{vv} = 0, \quad \kappa_1 \neq 0, \quad \rho_v \neq 0,
$$

$$
-b_1\rho_u + a_1\gamma_{uu} \neq 0, \quad d_{-1}\rho_u \neq 0, \quad a_1 \neq 0,
$$

$$
\begin{aligned}
\mathscr{D}_u &= \frac{-\kappa_2 + \rho_u}{\kappa_1}, \quad \mathscr{D}_v = -\frac{\kappa_2}{\kappa_1}, \quad \gamma_{uu} = \frac{\gamma_{vu}\rho_u}{\rho_v},\\
b_1 &= \frac{a_1\gamma_{vu}}{\rho_v}, \quad b_{-1} = \frac{a_{-1}\gamma_{uu}}{\rho_u},
\end{aligned}
$$

with a_{-1}, c_1, c_0 and κ_2 arbitrary constants. The corresponding exact solutions are given by

$$
U_{(1,2)}(\zeta) = \frac{a_{-1}e^{-\zeta} + a_1 e^{\zeta}}{(\frac{a_{-1}\gamma_{uu}}{\rho_u})e^{-\zeta} + (\frac{a_1\gamma_{vu}}{\rho_v})e^{\zeta}}, \qquad V_{(1,2)}(\zeta) = \frac{c_0 + c_1 e^{\zeta}}{d_{-1}e^{-\zeta}}.
$$

Case 3. A third solution branch is obtained under

$$\gamma_{vv}=0,\quad \gamma_{uv}=0,\quad c_1=0,\quad a_0=0,\quad b_0=0,$$

$$\gamma_{vu}\kappa_1\neq 0,\quad \gamma_{uu}\rho_v\neq 0,\quad d_{-1}\rho_v\neq 0,\quad \rho_u\neq 0,$$

$$\rho_u=\frac{\rho_v\gamma_{uu}}{\gamma_{vu}},\quad \mathscr{D}_u=\frac{-\gamma_{vu}\kappa_2+\gamma_{uu}\rho_v}{\gamma_{vu}\kappa_1},\quad \mathscr{D}_v=\frac{-\kappa_2}{\kappa_1},$$

$$b_{-1}=\frac{a_{-1}\gamma_{vu}}{\rho_v},\quad b_1=\frac{a_1\gamma_{uu}}{\rho_u},$$

with a_{-1}, a_1, c_{-1}, c_0, d_0, $d_1 and$ κ_2 arbitrary. The corresponding exact solutions are given by

$$U_{(1,3)}(\zeta)=\frac{a_{-1}e^{-\zeta}+a_1e^{\zeta}}{(\frac{a_{-1}\gamma_{vu}}{\rho_v})e^{-\zeta}+(\frac{a_1\gamma_{uu}}{\rho_u})e^{\zeta}},\qquad V_{(1,3)}(\zeta)=\frac{c_{-1}e^{-\zeta}+c_0}{d_{-1}e^{-\zeta}+d_0+d_1e^{\zeta}}.$$

Case 4. The final admissible solution branch is obtained for

$$\gamma_{vv}=0,\quad \gamma_{uv}=0,\quad \gamma_{vu}\neq 0,\quad \kappa_1\neq 0,$$

$$b_1c_1d_1\rho_u\neq 0,\quad c_{-1}\rho_u\neq 0,\quad d_{-1}\rho_v\neq 0,$$

$$\rho_u=\frac{\rho_v\gamma_{uu}}{\gamma_{vu}},\quad \mathscr{D}_u=-\frac{\kappa_2}{\kappa_1},\quad \gamma_{uu}=\frac{\gamma_{vu}\rho_u}{\rho_v},$$

$$b_{-1}=\frac{a_{-1}\gamma_{vu}}{\rho_v},\quad b_0=\frac{a_0\gamma_{uu}}{\rho_u},\quad c_0=\frac{c_1d_0}{d_1},\quad c_1=\frac{c_{-1}d_1}{d_{-1}},\quad a_1=\frac{b_1\rho_u}{\gamma_{uu}},$$

with c_{-1}, b_1, a_0, a_{-1}, d_{-1}, d_0, d_1, and κ_2 being arbitrary constants. The corresponding exact solutions are given by

$$U_{(1,4)}(\zeta)=\frac{a_{-1}e^{-\zeta}+a_0+\left(\frac{b_1\rho_u}{\gamma_{uu}}\right)e^{\zeta}}{\left(\frac{a_{-1}\gamma_{vu}}{\rho_v}\right)e^{-\zeta}+\left(\frac{a_0\gamma_{uu}}{\rho_u}\right)+b_1e^{\zeta}},\qquad V_{(1,4)}(\zeta)=\frac{c_{-1}e^{-\zeta}+\left(\frac{c_1d_0}{d_1}\right)+\left(\frac{c_{-1}d_1}{d_{-1}}\right)e^{\zeta}}{d_{-1}e^{-\zeta}+d_0+d_1e^{\zeta}}.$$

Verification of the obtained Exp–function solutions

To verify the validity of the obtained analytical solutions, all solution branches derived from the Exp–function method were substituted into the original fractional reaction–diffusion system (1).
Using the fractional traveling-wave transformation together with the adopted fractional derivative properties, the residual functions were defined as

$$R_u=D_t^{\alpha_t}u-\mathscr{D}_uD_x^{\alpha_x}u-(\rho_u-\gamma_{uu}u-\gamma_{uv}v)u,$$
$$R_v=D_t^{\alpha_t}v-\mathscr{D}_vD_x^{\alpha_x}v-(\rho_v-\gamma_{vv}v-\gamma_{vu}u)v.$$

The obtained expressions $U(\zeta)$ and $V(\zeta)$ were substituted into these residuals and simplified symbolically using *Mathematica*. As a representative example, substituting $U_{(1,1)}(\zeta)$ and $V_{(1,1)}(\zeta)$ into the above residual functions shows that both residuals vanish identically. The same verification procedure was applied to all remaining admissible solution branches.

For every admissible solution branch reported in this section, the residuals were found to satisfy

$$R_u \equiv 0, \qquad R_v \equiv 0.$$

Therefore, all reported Exp–function solutions satisfy the original fractional-order coupled system (1) exactly and not merely the reduced ordinary differential system (19).

The parameter values used in the figures are dimensionless and were selected solely to illustrate the qualitative behavior of the obtained analytical solutions. They are not intended to represent a specific biological system.

To illustrate the qualitative features of the obtained solutions, several representative profiles are presented in the following figures.

5 Conclusion

In this work, the Exp–function method combined with the rational $\frac{G'}{G}$–expansion method was employed to derive exact analytical solutions of space–time FDEs relevant to ecological and population dynamics models. The obtained solutions encompass various functional forms, including hyperbolic, rational, and soliton-like structures. To assess the qualitative behavior and validate the results, both two- and three-dimensional graphical simulations were conducted.

The findings reveal that fractional-order formulations capture the inherent complexity of ecological invasion processes more effectively than classical integer-order models, accurately representing spatial and temporal heterogeneity. The derived soliton-type solutions underscore the utility of fractional derivatives in modeling species dispersal and interaction dynamics. By integrating fractional calculus with advanced expansion techniques, this approach not only provides closed-form analytical solutions but also deepens the theoretical understanding of nonlinear ecological systems.

Overall, these results demonstrate the versatility and reliability of fractional models in representing real-world ecological scenarios. Future research could extend this framework to higher-dimensional fractional systems and more intricate ecological settings, including multi-species interactions, predator–prey dynamics, and resource-limited environments. This study highlights the potential of fractional-order modeling to advance both theoretical insights and practical applications in applied mathematics, ecology, and related disciplines.

Acknowledgements

We would like to express our sincere thanks to referees for helpful advice and suggestions.

Conflict of Interest

The authors declare no competing financial interests or personal relationships that could have influenced this work.

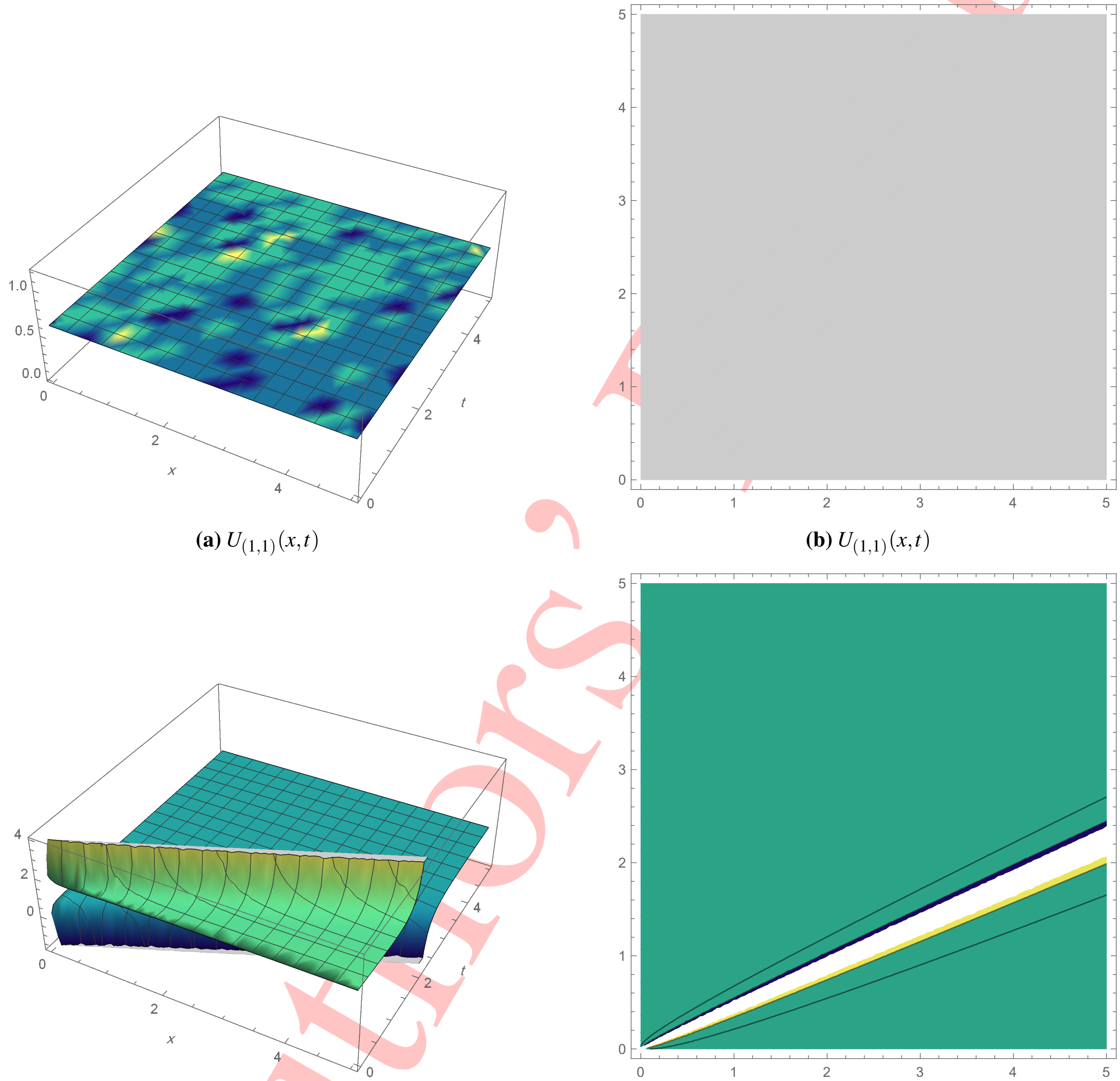

(a) $U_{(1,1)}(x,t)$ **(b)** $U_{(1,1)}(x,t)$

(c) $V_{(1,1)}(x,t)$ **(d)** $V_{(1,1)}(x,t)$

Figure 5: Two- and three-dimensional profiles of the exact solutions $U_{(1,1)}(x,t)$ and $V_{(1,1)}(x,t)$ corresponding to Case 1 of the Exp–function method

Table 4: Dimensionless parameter values used to generate Figure 5

Parameter	α_x	α_t	a_{-1}	c_{-1}	c_0	b_1	d_1	d_{-1}	γ_{vu}	γ_{uu}	ρ_v	κ_1	κ_2	x	t
Value	1/2	1/2	7	-2	1	2	8	-4	5	4	3	2	3	(0,5)	(0,5)

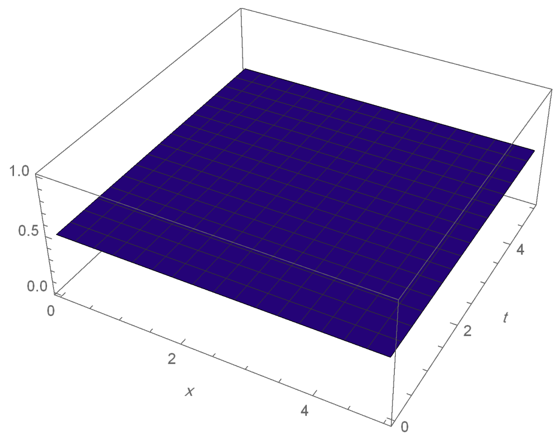

(a) $U_{(1,2)}(x,t)$

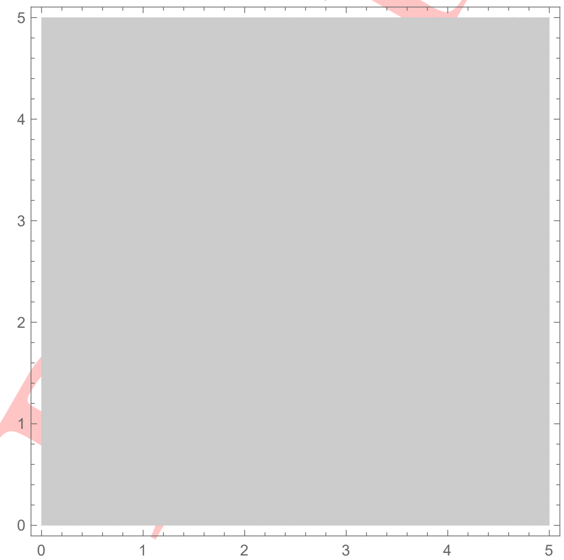

(b) $U_{(1,2)}(x,t)$

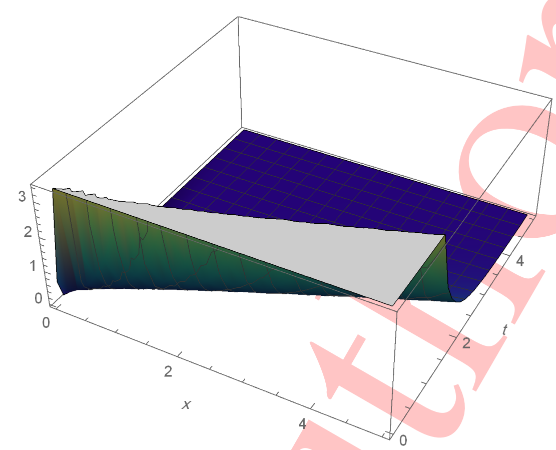

(c) $V_{(1,2)}(x,t)$

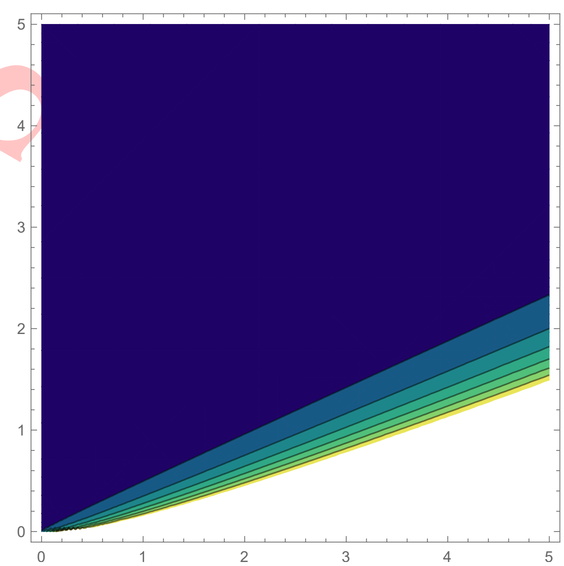

(d) $V_{(1,2)}(x,t)$

Figure 6: Two- and three-dimensional profiles of the exact solutions $U_{(1,2)}(x,t)$ and $V_{(1,2)}(x,t)$ corresponding to Case 2 of the Exp–function method

Table 5: Dimensionless parameter values used to generate Figure 6

Parameter	α_x	α_t	a_{-1}	a_1	c_0	c_1	d_{-1}	γ_{vu}	γ_{uu}	ρ_u	ρ_v	κ_1	κ_2	x	t
Value	0.5	0.5	7	3	1	4	8	5	4	2	3	2	3	(0,5)	(0,5)

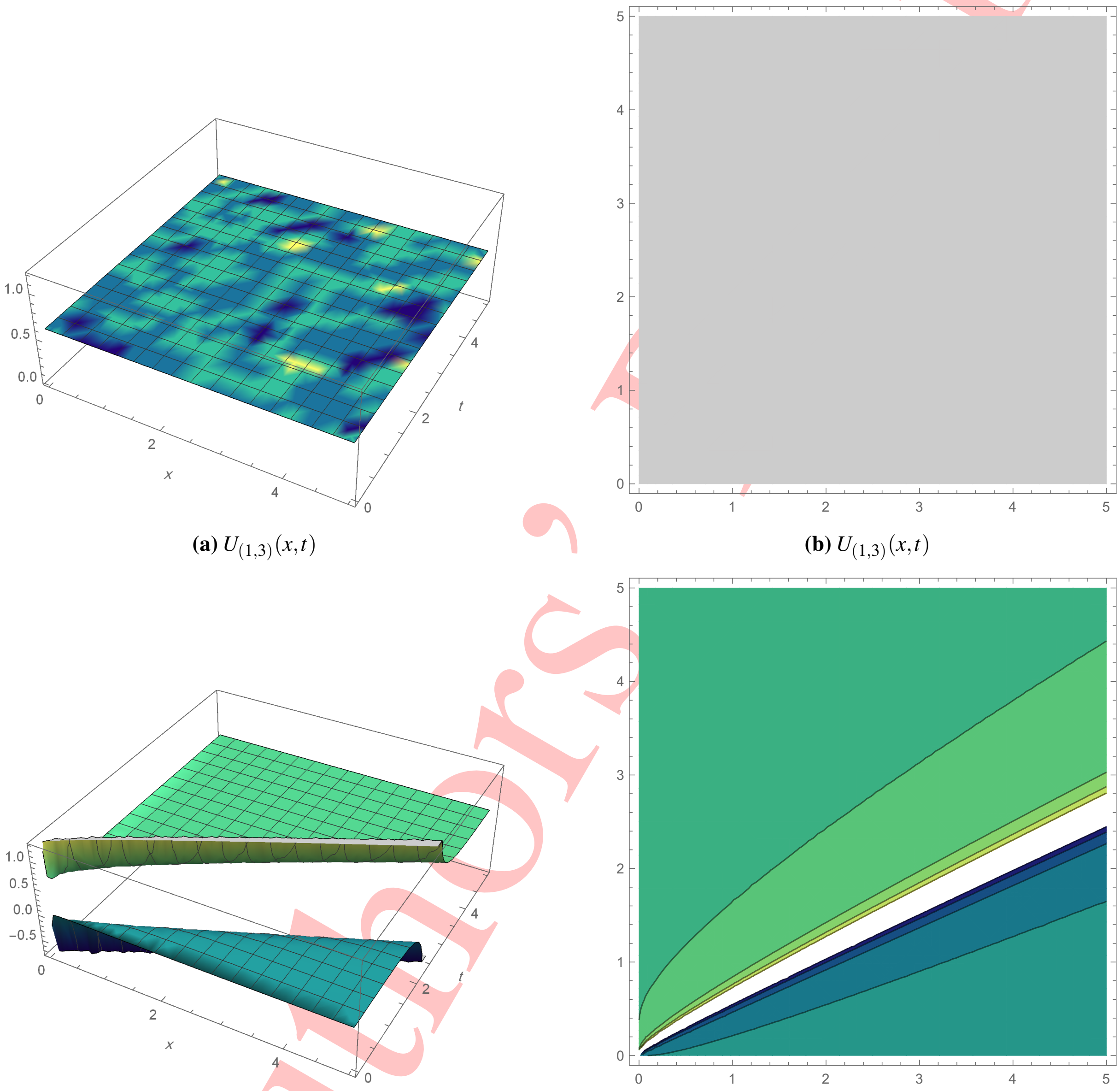

(a) $U_{(1,3)}(x,t)$ **(b)** $U_{(1,3)}(x,t)$

(c) $V_{(1,3)}(x,t)$ **(d)** $V_{(1,3)}(x,t)$

Figure 7: Two- and three-dimensional profiles of the exact solutions $U_{(1,3)}(x,t)$ and $V_{(1,3)}(x,t)$ corresponding to Case 3 of the Exp–function method

Table 6: Dimensionless parameter values used to generate Figure 7

Parameter	α_x	α_t	a_{-1}	a_1	c_0	c_{-1}	d_{-1}	d_0	d_1	γ_{vu}	γ_{uu}	ρ_v	κ_1	κ_2	x	t
Value	0.5	0.5	7	3	1	-2	-4	1	8	5	4	3	2	3	(0,5)	(0,5)

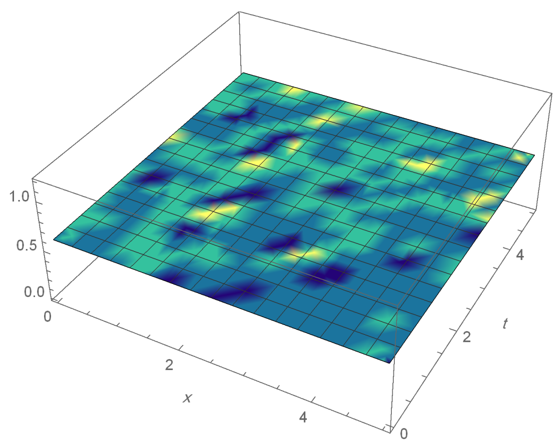

(a) $U_{(1,4)}(x,t)$

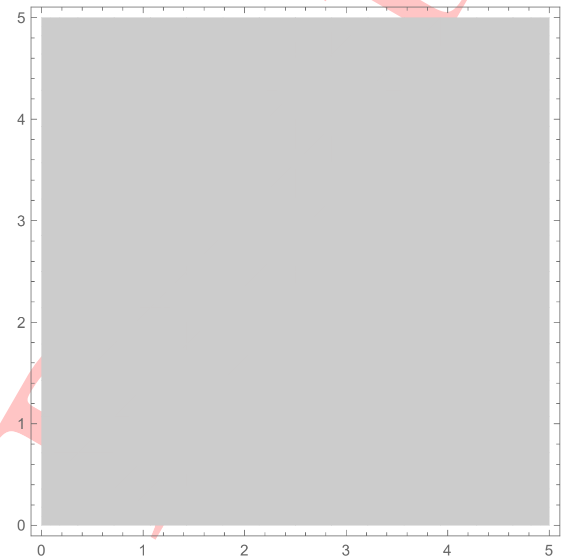

(b) $U_{(1,4)}(x,t)$

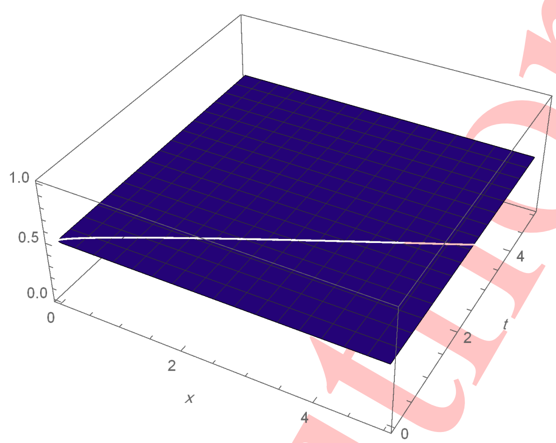

(c) $V_{(1,4)}(x,t)$

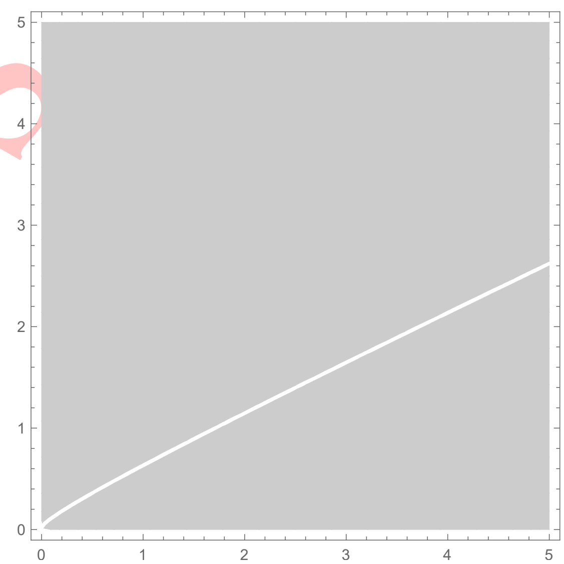

(d) $V_{(1,4)}(x,t)$

Figure 8: Two- and three-dimensional profiles of the exact solutions $U_{(1,4)}(x,t)$ and $V_{(1,4)}(x,t)$ corresponding to Case 4 of the Exp–function method

Table 7: Dimensionless parameter values used to generate Figure 8

Parameter	α_x	α_t	a_{-1}	a_0	b_1	c_{-1}	d_{-1}	d_0	d_1	γ_{vu}	γ_{uu}	ρ_v	κ_1	κ_2	x	t
Value	1/2	1/2	7	1	2	-2	-4	1	8	5	4	3	2	3	(0,5)	(0,5)

References

[1] I. Ali, S. Islam, *Stability analysis of fractional two-dimensional reaction–diffusion model with applications in biological processes*, AIMS Math. **10** (2025) 11732–11756.

[2] M.A. Akbar, N.H. M. Ali, M.T. Islam, *Multiple closed form solutions to some fractional order nonlinear evolution equations in physics and plasma physics*, AIMS Math. **4** (2019) 397–411.

[3] M. Bilal, J. Iqbal, K. Shah, B. Abdalla, T. Abdeljawad, I. Ullah, *Analytical solutions of the space–time fractional Kundu–Eckhaus equation by using modified extended direct algebraic method*, Partial Differ. Equ. Appl. Math. **11** (2024) 100832.

[4] K. Diethelm, *The Analysis of Fractional Differential Equations*, Springer, Berlin, 2010.

[5] A. Ebaid, *An improvement on the Exp-function method when balancing the highest order linear and nonlinear terms*, J. Math. Anal. Appl. **392** (1) (2012) 1–5.

[6] T. Elghareb, S.K. Elagan, Y.S. Hamed, M. Sayed, *An exact solutions for the generalized fractional Kolmogorov–Petrovskii–Piskunov equation by using the generalized* $\left(\frac{G'}{G}\right)$*-expansion method*, Int. J. Basic Appl. Sci. **13** (2013) 19–22.

[7] S.M. Elnady, M.A. El-Beltagy, M.E. Fouda, A.G. Radwan, *The chain rule for fractional-order derivatives: Theories, challenges, and unifying directions*, AppliedMath **6** (2026) 25.

[8] A. Ghafoor, M.R. Khan, S. Ahmed, *Dynamics of the time-fractional reaction–diffusion coupled equations in biological and chemical processes*, Sci. Rep. **14** (2024) 58073.

[9] J.H. He, *Homotopy perturbation technique*, Comput. Methods Appl. Mech. Eng. **178** (1999) 257–262.

[10] J.H. He, S.K. Elagan, Z.B. Li, *Geometrical explanation of the fractional complex transform and derivative chain rule for fractional calculus*, Phys. Lett. A **376** (2013) 257–259.

[11] E. Holmes, M. Lewis, J. Banks, R. Veit, *Partial differential equations in ecology: Spatial interactions and population dynamics*, Ecology **75** (1994) 17–29.

[12] R. Hirota, *Exact solution of the Korteweg–de Vries equation for multiple collisions of solitons*, Phys. Rev. Lett. **27** (1971) 1192–1194.

[13] G. Jumarie, *Modified Riemann–Liouville derivative and fractional Taylor series of non-differentiable functions: Further results*, Comput. Math. Appl. **51** (2006) 1367–1376.

[14] G. Jumarie, *Modified Riemann–Liouville derivative: New methods for solution of fractional differential equations*, Math. Comput. Model. **24** (2007) 31–48.

[15] G. Jumarie, *Table of some basic fractional calculus formulae derived from a modified Riemann–Liouville derivative for non-differentiable functions*, Appl. Math. Lett. **22** (2009) 378–385.

[16] A.A. Kilbas, H.M. Srivastava, J.J. Trujillo, *Theory and Applications of Fractional Differential Equations*, Elsevier, Amsterdam, 2006.

[17] Z.B. Li, J.H. He, *Fractional complex transform for fractional differential equations*, Math. Comput. Appl. **15** (2010) 970–975.

[18] M.A. Lewis, P. Kareiva, *Allee dynamics and the spread of invading organisms*, Theor. Popul. Biol. **43** (1993) 141–158.

[19] R.L. Magin, *Fractional Calculus in Bioengineering*, Begell House, New York, 2006.

[20] H. Mesgarani, A. Adl, and Y. Esmaeelzade Aghdam, *Approximate price of the option under discretization by applying quadratic interpolation and Legendre polynomials*, Mathematical Sciences **17** (2023) 51–58.

[21] R. Metzler, J. Klafter, *The random walk's guide to anomalous diffusion: A fractional dynamics approach*, Phys. Rep. **339** (2000) 1–77.

[22] S. Petrovskii, A. Morozov, *Wave of chaos: New mechanism of pattern formation in population dynamics*, Theor. Popul. Biol. **59** (2001) 157–174.

[23] I. Podlubny, *Fractional Differential Equations*, Academic Press, San Diego, 1999.

[24] R. Rahul, R. Kumar, A. Bansal, S. Kumar, *Symmetry reductions and qualitative analysis of time fractional K(m,1) equation*, Partial Differ. Equ. Appl. Math. **6** (2023) 100448.

[25] R. Rahmatullah, R. Ellahi, S.T. Mohyud-Din, U. Khan, *Exact traveling wave solutions of fractional order Boussinesq-like equations by applying Exp-function method*, Results Phys. **8** (2018) 114–120.

[26] J. Rashidinia, A. Momeni, *Collocation method for solving fractional reaction–diffusion problem arising in chemistry*, Sci. Rep. **15** (2025) 53339.

[27] D.U. Sarwe, A.S. A. Raj, P. Kumar, S. Salahshour, *A novel analysis of the fractional Cauchy reaction–diffusion equations*, Indian J. Phys. **99** (2025) 1825–1837.

[28] J.G. Skellam, *Random dispersal in theoretical populations*, Biometrika **38** (1951) 196–218.

[29] V.E. Tarasov, *On chain rule for fractional derivatives*, Commun. Nonlinear Sci. Numer. Simul. **30** (2016) 1–4.

[30] Y. Tian, J. Liu, *A modified Exp-function method for fractional partial differential equations*, Thermal Sci. **25** (2021) 1237–1241.

[31] Q. Wang, *Numerical solutions for fractional KdV–Burgers equation by Adomian decomposition method*, Appl. Math. Comput. **182** (2) (2006) 1048–1055.

[32] M. Wang, X. Li, J. Zhang, *The Exp-function method for nonlinear evolution equations*, Chaos Solit. Fractals **38** (2008) 896–905.

[33] J. Zhang, J. Wei, X. Lu, *The (G'/G)-expansion method for traveling wave solutions of nonlinear evolution equations*, Appl. Math. Comput. **182** (2007) 495–502.

[34] G. M. Zaslavsky, *Chaos, fractional kinetics, and anomalous transport*, Phys. Rep. **371** (2002) 461–580.

[35] A. Zulfiqar, J. Ahmad, *Soliton solutions of fractional modified unstable Schrödinger equation using Exp-function method*, Results Phys. **19** (2020) 103476.